bioRxiv preprint doi: https://doi.org/10.1101/2025.05.04.652152; this version posted May 6, 2025. The copyright holder for this preprint (which was not certified by peer review) is the author/funder, who has granted bioRxiv a license to display the preprint in perpetuity. It is made available under a CC-BY 4.0 International license.

Common garden experiments suggest terpene-mediated interactions between phyllosphere microbes and *Cryptomeria japonica*

Satoyoshi Ishizaki[1,*], Tetsuo I. Kohyama[1], Yuki Ota[1], Takuya Saito[2], Yoshihisa Suyama[3], Yoshihiko Tsumura[4], Tsutom Hiura[1]

[1] Department of Ecosystem Studies, Graduate School of Agricultural and Life Sciences, The University of Tokyo, Tokyo 113-8657, Japan

[2] National Institute for Environmental Studies, Tsukuba 305-8506, Japan

[3] Field Science Center, Graduate School of Agricultural Science, Tohoku University, Osaki 989-6711, Japan

[4] Institute of Life and Environmental Sciences, University of Tsukuba, Tsukuba 305-8572, Japan

* Corresponding author: ishizaki-satoyoshi766@g.ecc.u-tokyo.ac.jp

bioRxiv preprint doi: https://doi.org/10.1101/2025.05.04.652152; this version posted May 6, 2025. The copyright holder for this preprint (which was not certified by peer review) is the author/funder, who has granted bioRxiv a license to display the preprint in perpetuity. It is made available under a CC-BY 4.0 International license.

Abstract

Plant–microbe interactions in the phyllosphere provide invaluable information on plant ecology, with implications for ecosystem functioning and plant–atmosphere feedbacks. The composition of phyllosphere microbial communities varies significantly depending on host lineages, geographic regions, and climatic conditions. However, the factors driving these variations in interactions with plants remain poorly understood. Biogenic volatile organic compounds (BVOCs) emitted by plants may be important in these interactions. Here, we quantified the composition of phyllosphere microbial communities and terpene emissions from leaves of Japanese cedar (*Cryptomeria japonica*) trees grown in two common gardens from cuttings collected from natural populations across Japan. Amplicon sequencing revealed that bacterial and fungal communities differed significantly between gardens and among host population origins. Analysis of BVOC profiles showed that the camphene emission rate was associated with bacterial community composition, whereas that of β-farnesene was linked to fungal community composition. The relative abundances of certain putative plant pathogens and the emission rates of most monoterpenes were correlated with the climatic conditions at the origin sites of cedar trees. These findings highlight the intricate relationships between phyllosphere microbial communities and terpene emission from host trees and suggest the role of climatic factors in shaping these interactions.

bioRxiv preprint doi: https://doi.org/10.1101/2025.05.04.652152; this version posted May 6, 2025. The copyright holder for this preprint (which was not certified by peer review) is the author/funder, who has granted bioRxiv a license to display the preprint in perpetuity. It is made available under a CC-BY 4.0 International license.

Introduction

The aerial surface of plant leaves, called the phyllosphere, harbors a diverse array of microbes including bacteria and fungi[1]. Interactions between phyllosphere microbes and host plants have a considerable impact on plant physiology and ecology. Phyllosphere microbes can influence plant fitness by causing or suppressing disease[2–5] or by promoting plant growth and stress tolerance[6,7]. Plant defense against pathogens and the counteradaptation by the latter further complicate plant–microbe interactions[7–10]. Studies have even suggested that these interactions contribute to ecosystem functioning, including nutrient cycling[11–15] and ecosystem productivity[12,15,16]. Microbial infection may also affect plant–atmosphere feedbacks through microbial metabolization of gases emitted by plants[14,17–19]. Studies of plant–microbe interactions can lead to insights into key issues in ecology, such as the evolution of plant traits, drivers of ecosystem functions, and biosphere–atmosphere interactions.

Shifts in the composition of the phyllosphere microbial community are significant indicators of changes in plant–microbe interactions[5,15,20]. This composition is affected by environmental factors including climate[21,22], season[21,23], land use[24,25], location[21,26], and geographic distance[24] as well as by host-related factors such as species[21,27,28] and traits[21,29]. The effect of host genotypes on microbial composition in the phyllosphere has been investigated using known characterized mutants or accessions[23,26,30]. However, further

bioRxiv preprint doi: https://doi.org/10.1101/2025.05.04.652152; this version posted May 6, 2025. The copyright holder for this preprint (which was not certified by peer review) is the author/funder, who has granted bioRxiv a license to display the preprint in perpetuity. It is made available under a CC-BY 4.0 International license.

55 investigation of genetic and phenotypic variation within wild plant species is necessary to
56 elucidate the interactions and coevolution of phyllosphere microbes with plants.

57 Biogenic volatile organic compounds (BVOCs) are plant-derived secondary metabolites
58 that affect plant–microbe interactions[10,31]. BVOCs affect plant resistance to microbes by
59 directly inhibiting microbial growth by damaging microbial cell membranes[32,33] and inducing
60 plant immune responses[34]. On the other hand, some microbes metabolize BVOCs stored in or
61 emitted from plants and use them as a carbon source, suggesting their adaption to plant
62 resistance mechanisms[13,14,35,36]. While many laboratory studies have suggested a relationship
63 between pathogen-induced BVOC emission by plants and phyllosphere microbes[34,37,38], few
64 have investigated the roles of constitutive BVOC emission by plants under natural conditions
65 in plant–microbe interactions[39,40]. Significant inter- and intraspecific variations in both the
66 composition of the phyllosphere microbial community and emission rates of BVOCs have
67 been reported for wild plants[39,41,42]. Elucidating the drivers and interrelationships of these
68 variations is a challenge in understanding plant–microbe interactions mediated by plant
69 BVOC emission.

70 BVOC emission can also have a significant impact on atmospheric chemical processes
71 and climate. Oxidation of emitted BVOCs can indirectly affect the radiative balance by
72 increasing the lifetime of certain greenhouse gases due to a decrease in oxidative capacity in
73 the atmosphere[43]. Secondary organic aerosols produced by BVOC oxidation act as cloud
74 condensation nuclei and may affect regional climate[44]. Guenther et al.[45] estimated that

bioRxiv preprint doi: https://doi.org/10.1101/2025.05.04.652152; this version posted May 6, 2025. The copyright holder for this preprint (which was not certified by peer review) is the author/funder, who has granted bioRxiv a license to display the preprint in perpetuity. It is made available under a CC-BY 4.0 International license.

terrestrial plants emit about 1 billion tons of BVOCs per year, of which about 92% is emitted by forest trees. These estimates are based on the model of the standardized rates of BVOC emission by plants. However, this model does not fully account for variations in the amounts and composition of emitted BVOCs among and within plant species or the influences of plant interactions with microbes. Therefore, elucidating the relationship between plant–microbe interactions and plant BVOC emissions is important for understanding the plant–aerosol–climate feedbacks.

Wild populations of Japanese cedar, *Cryptomeria japonica* (Cupressaceae), are widely distributed in Japan, ranging from Yakushima Island, the southern limit of their distribution, to the northern limit of Ajigasawa (Aomori Prefecture)[46] (Supplementary Fig. S1 and Table S1). As one of the major silvicultural tree species in Japan, *C. japonica* accounts for approximately 20% of the total forest area, including plantations[47].

Japanese cedar emits substantial amounts of terpenes, including monoterpenes (MTs), sesquiterpenes (SQTs), and diterpenes (DTs)[48–50]. In comparison with MTs, SQTs and DTs have high molecular weights and are highly reactive in the atmosphere[51,52]. Considering the large numbers of *C. japonica* in Japan's forests, these terpenes may have a non-negligible impact on the surrounding atmospheric environment. A study based on a common garden experiment reported significant intraspecific variation in the composition of terpenes stored in and emitted from the leaves of Japanese cedars[50]. Intraspecific genetic variation in Japanese cedar has been well studied, revealing a geographic genetic structure with four main

bioRxiv preprint doi: https://doi.org/10.1101/2025.05.04.652152; this version posted May 6, 2025. The copyright holder for this preprint (which was not certified by peer review) is the author/funder, who has granted bioRxiv a license to display the preprint in perpetuity. It is made available under a CC-BY 4.0 International license.

95 clades: the Pacific Ocean side clade, two Sea of Japan side clades, and the Yakushima Island
96 clade[53–55].

97 Intraspecific variation in physiological and morphological traits of Japanese cedar has
98 been revealed by common garden experiments, suggesting adaptation to the original
99 environments[56–58]. The reasons for differences in the quantity and composition of stored and
100 emitted terpenes among Japanese cedar populations are still unclear. However, these
101 differences may be influenced by the local climate and pathogen communities at the original
102 locations of the populations[50]. The problem is that the pathogen community data used in that
103 study were based on previously published information, and no quantitative data were
104 obtained on the actual microbial community on the leaf surface of Japanese cedar. To clarify
105 whether the intraspecific variations in terpene emissions observed in this species reflect the
106 variations in the phyllosphere microbial community, quantitative investigations of both
107 microbial communities and BVOCs emitted by the host are necessary.

108 Here, we investigated the phyllosphere microbial communities of Japanese cedar by
109 amplicon sequencing using cedar trees that have genetic variations and are grown in two
110 common gardens. We also measured terpene emission rates in some of these trees in one
111 common garden. Our objectives were (1) to clarify the variation in the phyllosphere microbial
112 community composition among Japanese cedar populations, and (2) to elucidate the
113 relationship between terpene emission rates and these microbial compositions. Our study

bioRxiv preprint doi: https://doi.org/10.1101/2025.05.04.652152; this version posted May 6, 2025. The copyright holder for this preprint (which was not certified by peer review) is the author/funder, who has granted bioRxiv a license to display the preprint in perpetuity. It is made available under a CC-BY 4.0 International license.

provides new insights into the mechanisms of plant–microbe interactions mediated by host-emitted BVOCs.

Results

Composition of the phyllosphere microbial community of Japanese cedar

Amplicon sequencing identified 2933 bacterial amplicon sequence variants (ASVs) and 5040 fungal ASVs across all samples from the phyllosphere microbial communities of Japanese cedar planted in the common gardens. After rarefaction, the richness of bacterial ASVs (9099 reads) was 89 ± 64 (mean ± SD) and that of fungal ASVs (17,427 reads) was 136 ± 121. In the bacterial communities, Proteobacteria (58.9% of all reads), Acidobacteriota (6.8%), Myxococcota (5.9%), Verrucomicrobiota (4.6%), Bacteroidota (3.0%), Firmicutes (2.5%), and Actinobacteriota (1.7%) were most abundant (Fig. 1a, b). The relative abundance of Myxococcota tended to be higher in the Kawatabi common garden, whereas that of Acidobacteriota was higher in the Tsukuba common garden. In the fungal communities, Dothideomycetes (32.4% of all reads), Eurotiomycetes (30.7%), Leotiomycetes (9.2%), Lecanoromycetes (7.6%), Sordariomycetes (2.6%), Cystobasidiomycetes (2.5%), Agaricomycetes (2.1%), and Tremellomycetes (1.8%) were most abundant (Fig. 1c, d). The relative abundance of Leotiomycetes and Lecanoromycetes tended to be higher in the Tsukuba common garden than in the Kawatabi common garden.

bioRxiv preprint doi: https://doi.org/10.1101/2025.05.04.652152; this version posted May 6, 2025. The copyright holder for this preprint (which was not certified by peer review) is the author/funder, who has granted bioRxiv a license to display the preprint in perpetuity. It is made available under a CC-BY 4.0 International license.

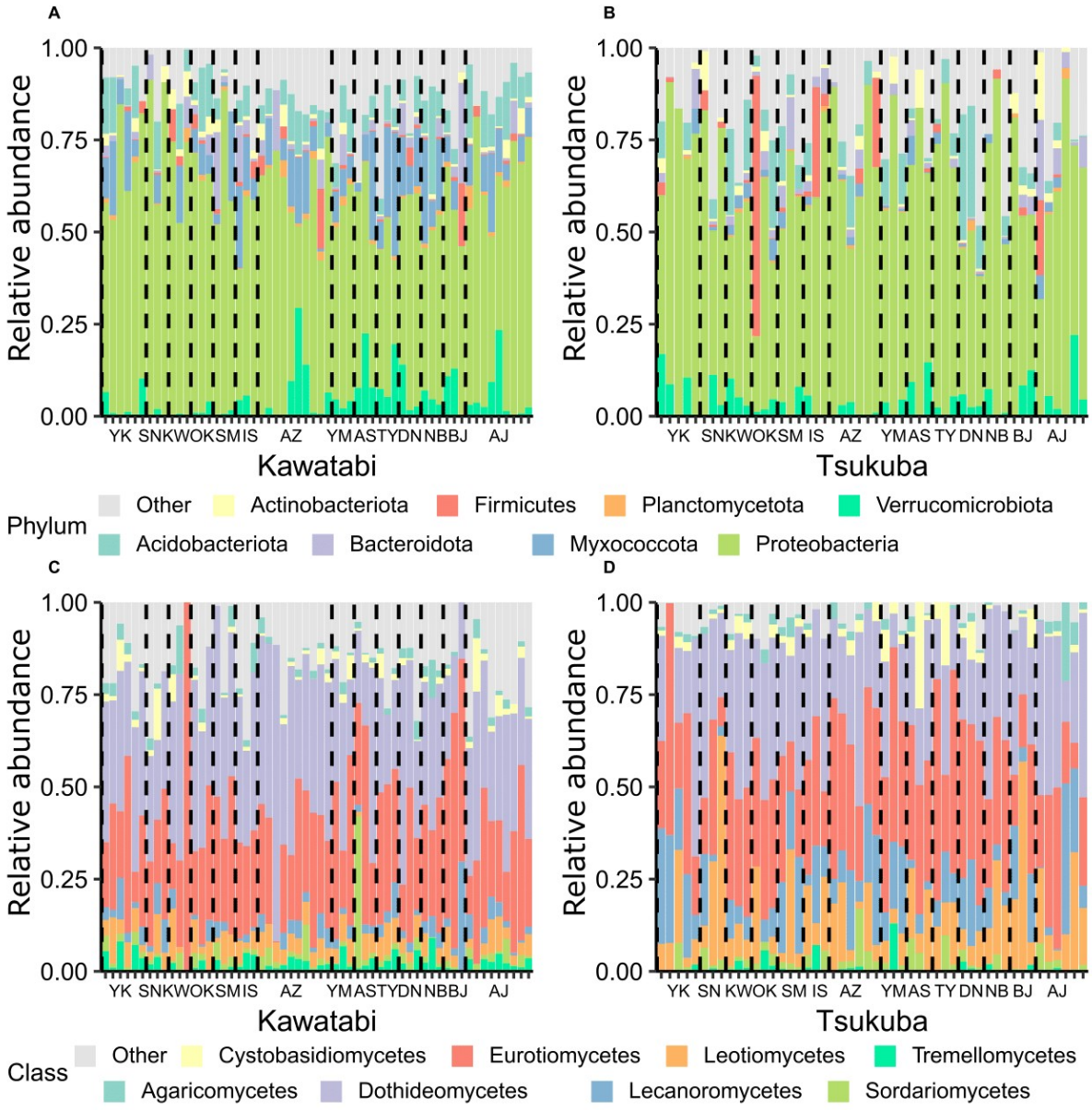


Figure 1

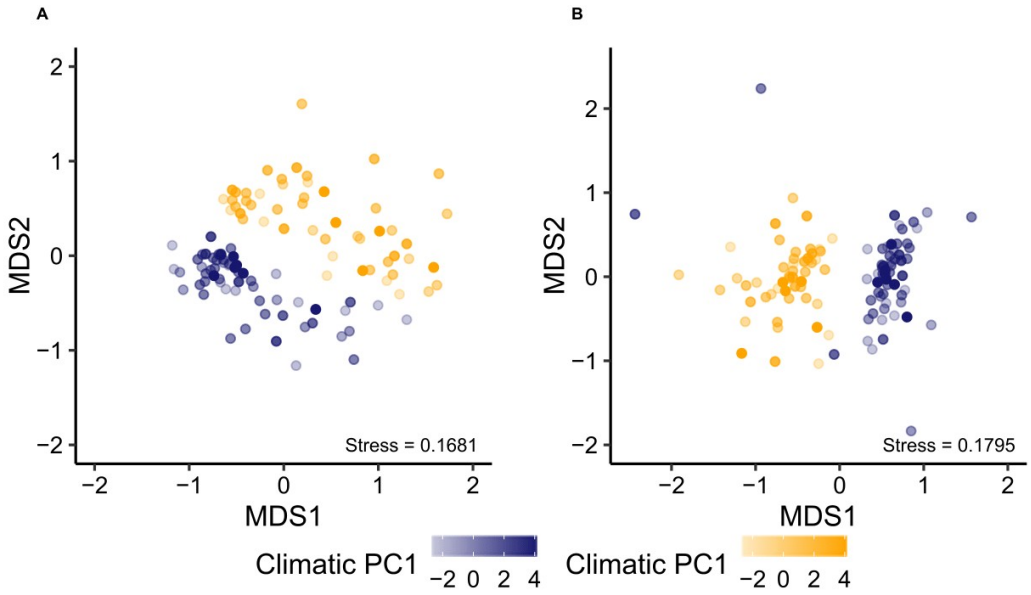
The composition of the bacterial and fungal communities was significantly influenced by the locations of the common gardens and host populations (Fig. 2). In the bacterial community, 38.3% of the total variation was explained by the common garden (PERMANOVA: $R^2 = 0.130$, $p = 0.001$), host population ($R^2 = 0.124$, $p = 0.014$), and their interaction ($R^2 = 0.128$, $p = 0.009$). In the fungal community, 40.1% of the total variation was

bioRxiv preprint doi: https://doi.org/10.1101/2025.05.04.652152; this version posted May 6, 2025. The copyright holder for this preprint (which was not certified by peer review) is the author/funder, who has granted bioRxiv a license to display the preprint in perpetuity. It is made available under a CC-BY 4.0 International license.

141 explained by the common garden (PERMANOVA: $R^2 = 0.176$, $p = 0.001$), host population

142 ($R^2 = 0.116$, $p = 0.028$), and their interaction ($R^2 = 0.115$, $p = 0.033$).

143



144

145 **Figure 2**

146

147 To investigate how climatic conditions at the original locations of the host populations

148 influence their effects on the composition of the microbial communities, we obtained the

149 climatic data[59–62] at these locations. A principal component analysis (PCA) of these data

150 revealed that 73.8% of the total variation was explained by the first two PCs (Supplementary

151 Fig. S2), which were used for the subsequent analysis. Climatic PC1, which explained

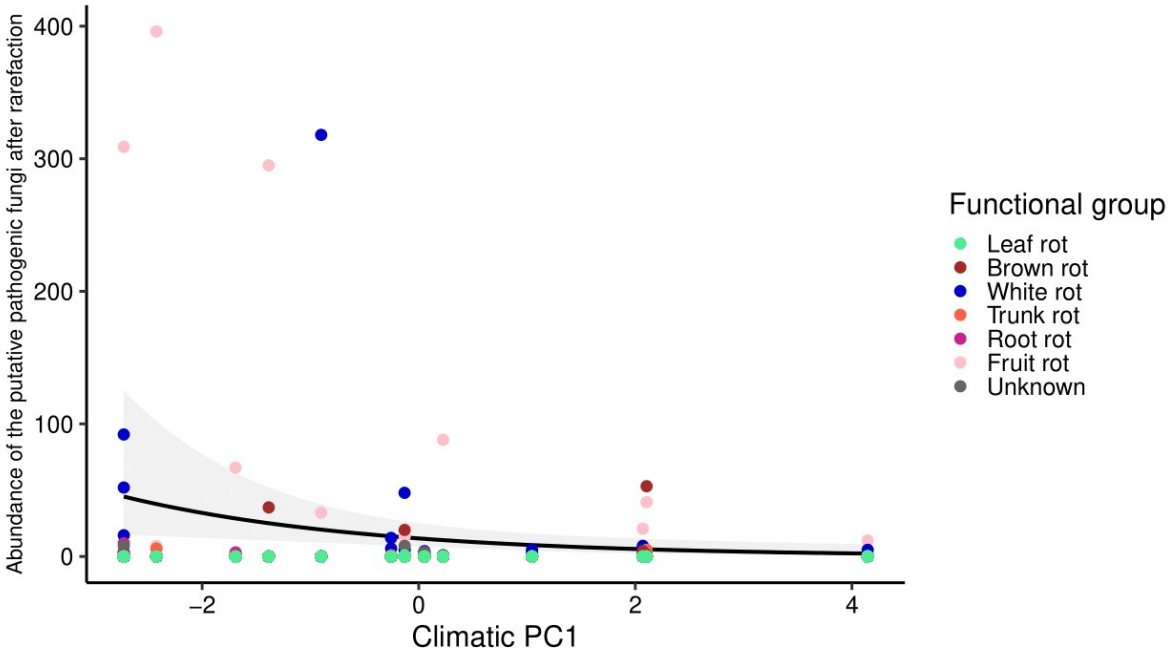
152 50.57% of the total variation, corresponded to higher annual mean temperature and mean

153 monthly potential evaporation and corresponded to lower standard deviation of the monthly

154 mean temperatures and the sum of the monthly precipitation for the months with mean

bioRxiv preprint doi: https://doi.org/10.1101/2025.05.04.652152; this version posted May 6, 2025. The copyright holder for this preprint (which was not certified by peer review) is the author/funder, who has granted bioRxiv a license to display the preprint in perpetuity. It is made available under a CC-BY 4.0 International license.

155 temperatures below 0 °C, suggesting that higher values of PC1 correspond to a warmer and
156 less snowy climate. Climatic PC2, which explained 23.19% of the total variation,
157 corresponded to higher mean monthly near-surface relative humidity and annual precipitation
158 and a lower coefficient of variation of the monthly precipitation estimates, suggesting that
159 higher values of PC2 correspond to higher amounts of precipitation and its stability.
160



161
162 **Figure 3**
163
164 The total explained variation in microbial community composition was reduced when
165 climatic PC1 and PC2 at the host origin sites were used as explanatory variables instead of
166 the host population. The result of PERMANOVA testing the effects of climatic PCs and their
167 interactions with the locations of the common gardens on the variation in bacterial
168 community composition was as follows: $R^2 = 0.014$ and $p = 0.044$ for PC1, $R^2 = 0.011$ and p

bioRxiv preprint doi: https://doi.org/10.1101/2025.05.04.652152; this version posted May 6, 2025. The copyright holder for this preprint (which was not certified by peer review) is the author/funder, who has granted bioRxiv a license to display the preprint in perpetuity. It is made available under a CC-BY 4.0 International license.

169 = 0.136 for the interaction between PC1 and common garden, R^2 = 0.009 and p = 0.335 for
170 PC2, R^2 = 0.010 and p = 0.160 for the interaction between PC2 and common garden. For the
171 total variation in fungal community composition, the result of PERMANOVA was R^2 = 0.010
172 and p = 0.126 for PC1, R^2 = 0.007 and p = 0.671 for the interaction between PC1 and
173 common garden, R^2 = 0.009 and p = 0.277 for PC2, and R^2 = 0.008 and p = 0.346 for the
174 interaction between PC2 and common garden. Of the detected fungal genera, 11 have been
175 described as Japanese cedar pathogens[63] (Supplementary Table S2). The aggregated
176 abundances of these putative pathogenic fungi after rarefaction were negatively correlated
177 with climatic PC1 at the host origin sites (Wald test: $\beta = -0.423 \pm 0.158$, $z = -2.676$, p =
178 0.007; Fig. 3); in particular, negative correlation was found for the abundances of white rot
179 fungi. However, the influence of common garden and climatic PC2 on these abundances was
180 not statistically significant (both $p > 0.1$).
181
182 **Relationships between terpene emissions, phyllosphere microbial community**
183 **composition, and climate**
184 Japanese cedar trees in the Kawatabi common garden emitted 12 MTs, one SQT, and one DT
185 (Fig. 4a). The DT was excluded from the subsequent analysis since only one tree emitted it.
186 PCA showed that PC1 and PC2 explained 70.8% of the total variation in the log-transformed
187 basal emission rates of terpenes (Fig. 4b). Terpene PC1 corresponded to higher basal
188 emission rates of most MTs and was significantly positively correlated with climatic PC1 and
189 PC2 at the tree origin sites (Student's t-test: climatic PC1, $\beta = 0.459 \pm 0.189$, t = 2.436, p =

bioRxiv preprint doi: https://doi.org/10.1101/2025.05.04.652152; this version posted May 6, 2025. The copyright holder for this preprint (which was not certified by peer review) is the author/funder, who has granted bioRxiv a license to display the preprint in perpetuity. It is made available under a CC-BY 4.0 International license.

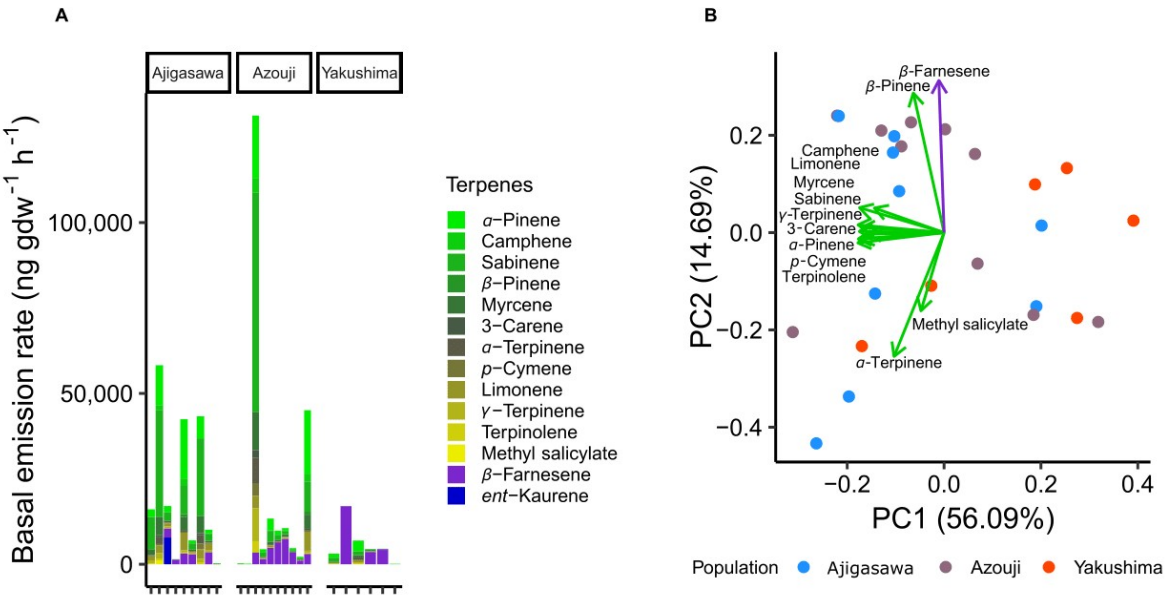
190 0.023; climatic PC2, $\beta = 0.874 \pm 0.417$, $t = 2.094$, $p = 0.047$; Supplementary Fig. S3).

191 Terpene PC2 corresponded to the higher basal emission rates of some MTs and β-farnesene

192 but was not significantly correlated with the climatic PCs (Student's t-test: climatic PC1, $\beta =$

193 -0.009 ± 0.108, $t = -0.084$, $p = 0.934$; climatic PC2, $\beta = -0.185 \pm 0.230$, $t = -0.803$, $p =$

194 0.430; Supplementary Fig. S3).



195

196 **Figure 4**

197

198 Significant correlations were detected between the basal emission rate of camphene and

199 bacterial community composition ($R^2 = 0.448$, $p = 0.003$; Fig. 5a). The sum of the basal

200 emission rates of MTs was marginally correlated with bacterial composition ($R^2 = 0.187$, $p =$

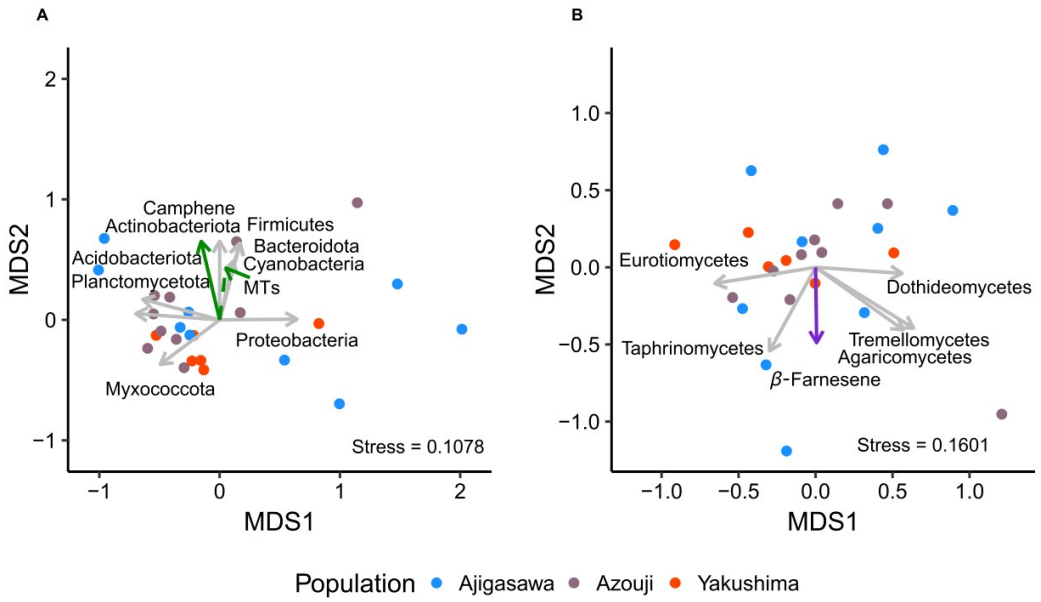
201 0.098). The basal emission rate of β-farnesene was significantly correlated with fungal

202 community composition ($R^2 = 0.239$, $p = 0.046$; Fig. 5b). The higher basal emission rate of

203 camphene and higher sum of the basal emission rates of MTs corresponded to higher

bioRxiv preprint doi: https://doi.org/10.1101/2025.05.04.652152; this version posted May 6, 2025. The copyright holder for this preprint (which was not certified by peer review) is the author/funder, who has granted bioRxiv a license to display the preprint in perpetuity. It is made available under a CC-BY 4.0 International license.

204 abundances of Actinobacteriota, Firmicutes, Bacteroidota, and Cyanobacteria. The higher
205 basal emission rate of β-farnesene corresponded to higher abundances of Taphrinomycetes,
206 Tremellomycetes, and Agaricomycetes.
207



208

209 **Figure 5**

210

211 **Discussion**

212 Using common garden experiments, we revealed differences in the composition of both
213 bacterial and fungal communities in the phyllosphere among wild populations of Japanese
214 cedar (Fig. 2). The data suggest that genetic variation among these populations influences
215 microbial composition in the phyllosphere. This result is consistent with those of previous
216 studies on grasses[23,26] and broad-leaved trees[64]. Although climate at the origin sites of cedar
217 populations explained only a relatively small proportion of the total variation in overall

bioRxiv preprint doi: https://doi.org/10.1101/2025.05.04.652152; this version posted May 6, 2025. The copyright holder for this preprint (which was not certified by peer review) is the author/funder, who has granted bioRxiv a license to display the preprint in perpetuity. It is made available under a CC-BY 4.0 International license.

218 microbial compositions, the relative abundances of putative pathogenic fungi were negatively
219 correlated with warm and less snowy climate at the host origin sites (Fig. 3), suggesting the
220 influence of climate on coevolution of some phyllosphere microbes and Japanese cedar.
221 Several studies have suggested a correlation between microbial community composition and
222 the environment, including climate[65–69]. It is possible that changes in distribution among
223 fungi coupled to climatic shifts may have influenced the coevolution of these fungi with
224 interacting plants. The relative abundances of the putative white rot fungal genera (*Trametes*,
225 *Phanerochaete*, *Pholiota*, and *Phellinus*) were negatively correlated with warmth at the host
226 origin sites (Fig. 3). Pathogens of these genera have been reported in wild Japanese cedar
227 populations, mainly in the northern region of Honshu Island[50], which is consistent with the
228 results of this study. Field-grown Japanese cedar trees from cold-climate populations have
229 been suggested to store higher amounts of terpenes[50], and these pathogens may be better
230 adapted than other microbes to this defense trait.
231 Our data suggest that the basal emission rates of some terpenes in Japanese cedar may be
232 related to the composition of the phyllosphere microbial community. The basal emission rate
233 of the MT camphene was correlated with the composition of the bacterial community (Fig.
234 5a). However, its amount was smaller than those of other terpenes such as α-pinene and
235 sabinene. The sum of the basal emission rates of MTs was also marginally correlated with
236 bacterial composition, and the direction of its loading vector was similar to that of camphene.
237 These results suggest the regulation of bacterial communities in the phyllosphere of Japanese

bioRxiv preprint doi: https://doi.org/10.1101/2025.05.04.652152; this version posted May 6, 2025. The copyright holder for this preprint (which was not certified by peer review) is the author/funder, who has granted bioRxiv a license to display the preprint in perpetuity. It is made available under a CC-BY 4.0 International license.

238 cedar by the emission of some MTs, possibly by that of camphene. The emission of multiple
239 terpenes is simultaneously induced by plant defense signaling pathways[10,17,70]. Camphene,
240 together with other MTs α-pinene and β-pinene, has been suggested to play a pivotal role in
241 the induction of defense responses against bacterial pathogens in *Arabidopsis thaliana*[34].
242 Given the correlation between the basal emission rate of camphene and those of most of the
243 other MTs (Fig. 4), multiple MTs may collectively control the bacterial communities on
244 Japanese cedar. It is also possible that the detection limits of terpene emission affected our
245 results, since many of the determined emission rates of camphene were low and this
246 compound was not detected in several samples. In addition, the outliers in the camphene
247 emission data may have influenced the correlation test. Furthermore, the small number of
248 populations used for BVOC measurements may have been a limiting factor, and further
249 investigation is needed.

250 The basal emission rate of the SQT β-farnesene was correlated with the composition of
251 the fungal community. The higher basal emission rate of the β-farnesene corresponded to the
252 higher relative abundances of Taphrinomycetes, Tremellomycetes, and Agaricomycetes (Fig.
253 5b). β-Farnesene is emitted upon insect herbivory in maize[71] and pathogen infection in
254 wheat[72]. Japanese cedar may also use β-farnesene as a defense substance against fungal
255 infection. Hiura et al.[50] suggested a correlation between the composition of the fungal
256 pathogen community in each cedar population and the relative basal emission rates of the
257 SQT α-farnesene and the DT *ent*-kaurene. Taken together, their data and the results of this

bioRxiv preprint doi: https://doi.org/10.1101/2025.05.04.652152; this version posted May 6, 2025. The copyright holder for this preprint (which was not certified by peer review) is the author/funder, who has granted bioRxiv a license to display the preprint in perpetuity. It is made available under a CC-BY 4.0 International license.

study suggest that Japanese cedar may be adapting to fungal biotic stresses by using relatively high-molecular-weight terpenes such as SQTs and DTs.

Some microbes are able to regulate or use plant defenses[10,73]. Firmicutes was one of the bacterial phyla whose relative abundance was higher on the hosts with higher basal emission rate of camphene (Fig. 5a). Some strains of Firmicutes induce immunity in tomato and are relatively abundant in plants with enhanced defense[74]. The induction of plant immunity often leads to the emission of terpenes[17,34,70]. However, the elevated level of camphene emission observed in this study may not be induced by bacteria, as the MTs emitted by Japanese cedar were suggested to be released primarily from storage pools[75]. Nevertheless, the possibility remains that Firmicutes may tolerate cedar defenses mediated by enhanced camphene emission. Taphrinomycetes, whose relative abundance was positively related to the basal emission rate of *β*-farnesene (Fig. 5b), include the genus *Taphrina*. All known *Taphrina* species are plant pathogens[76] and have various functional genes required for plant infection by these fungi, such as genes encoding enzymes involved in plant hormone biosynthesis or degradation of plant cell walls[77]. The positive correlations between the relative abundances of these microbes and the emissions of some terpenes may indicate microbial adaptation to the phyllosphere environment of Japanese cedar. Further investigation is needed to identify the microbial functions that support the BVOC-mediated interaction with the cedar.

We demonstrated that the locations of common gardens were the primary factor influencing microbial composition in the phyllosphere of Japanese cedar (Fig. 2). Multiple

bioRxiv preprint doi: https://doi.org/10.1101/2025.05.04.652152; this version posted May 6, 2025. The copyright holder for this preprint (which was not certified by peer review) is the author/funder, who has granted bioRxiv a license to display the preprint in perpetuity. It is made available under a CC-BY 4.0 International license.

278 factors may contribute to the observed differences in microbial composition between the
279 gardens. Geographic distance may affect the community assembly of local microbes,
280 particularly those with limited dispersal capabilities[24,68]. Fungi have larger spores[78] and are
281 more limited in dispersal than bacteria[68,79,80], which may explain the greater effect of
282 common garden on the fungal composition in this study. The two gardens differed in their
283 local environments since they are located at different latitudes and the surrounding land use is
284 also very different: Kawatabi is surrounded by a forest, whereas Tsukuba is surrounded by
285 farmland and an urban area. These differences in the local environment, such as climate[21,22]
286 and land use[24,81], may also have influenced the microbial composition in the gardens.
287 Although relatively few populations were used, our study suggested a negative correlation
288 between the basal emission rates of most MTs and warm, humid, and less snowy climates at
289 the original locations of the populations. Hiura et al.[50] suggested that the amounts of stored,
290 but not emitted, MTs in Japanese cedar are negatively correlated with warm and less snowy
291 climates, suggesting the existence of climate clines. Partial pressure calculated from the
292 stored amounts of MTs in Japanese cedar was suggested to be positively correlated with their
293 emission rates from the same leaf[75]. Therefore, the similar pattern of variations among
294 Japanese cedar populations in stored and emitted MTs may be attributed to the emission of
295 MTs from storage pools in leaves. We expect that consideration of both abiotic and biotic
296 environmental conditions will further our understanding of the mechanisms of BVOC
297 emission in plants in natural environments.

bioRxiv preprint doi: https://doi.org/10.1101/2025.05.04.652152; this version posted May 6, 2025. The copyright holder for this preprint (which was not certified by peer review) is the author/funder, who has granted bioRxiv a license to display the preprint in perpetuity. It is made available under a CC-BY 4.0 International license.

298 In conclusion, our findings revealed differences in the phyllosphere microbial community
299 compositions of *C. japonica* both between the common gardens and among wild populations,
300 as well as the correlation between the compositions and basal emission rates of some terpenes
301 by host trees. The results also suggest that the local climate at the origin sites of the Japanese
302 cedar populations is a significant factor influencing variations in the phyllosphere microbial
303 communities and terpene emission rates in this species. This study is among the few to
304 demonstrate in outdoor settings the relationship between the emission patterns of BVOCs and
305 both abiotic and biotic environments in trees with substantial BVOC emissions. Further
306 investigation is required to elucidate the mechanisms of plant–microbe interactions mediated
307 by BVOC emission and the impact of biotic interactions on plant–atmosphere feedbacks.
308

309 **Methods**

310 **Sampling sites and collection of phyllosphere microbiome**

311 We collected leaves at a height of about 1.5 m from cedar trees (about 5–6 m tall) on 2 June
312 2023 in the common garden at Kawatabi Field Science Center, Tohoku University (38.78°N,
313 140.73°E) and on 26 June 2023 in the common garden in the Tsukuba Experimental Forest,
314 University of Tsukuba Mountain Science Center (36.11°N, 140.10°E). The trees had
315 originated from 14 wild populations (Supplementary Fig. S1 and Table S1) and were grown
316 from cuttings in the common gardens. Leaves were collected from 3–10 individuals per
317 population (n = 108: Tsukuba = 50, Kawatabi = 58). Using scissors surface sterilized with
318 99% ethanol, leaves (ca. 5 g per tree) were collected in plastic bags, placed in cool bags with

bioRxiv preprint doi: https://doi.org/10.1101/2025.05.04.652152; this version posted May 6, 2025. The copyright holder for this preprint (which was not certified by peer review) is the author/funder, who has granted bioRxiv a license to display the preprint in perpetuity. It is made available under a CC-BY 4.0 International license.

ice packs, brought back to the laboratory within 1 day of collection, and stored at 4°C for one to two days.

Extraction of microbial DNA and amplicon sequencing

DNA of phyllosphere microbes was extracted using the protocol of Tian et al.[82] with modifications. Collected leaves were soaked in 40 mL of buffer (0.1 M potassium phosphate buffer with 0.1% Tween-80, pH 7.0) and microbes were separated from the leaf surface by sonication for 10 min in a Bransonic ultrasonic bath (Branson Ultrasonics, Danbury, CT, USA). Microbes were precipitated by centrifugation (10,000 ×*g*, 15 min) in a high-speed refrigerated microcentrifuge (Tomy, Nerima, Tokyo, Japan), suspended in 100 μL of PBS and stored at −20°C. DNA was extracted with a Fast DNA Spin Kit for Soil (MP Biomedicals, Irvine, CA, USA) following the manufacturer's protocol.

Bacterial and fungal DNA was amplified using Ex Taq Hot Start Version (Takara Bio, Kusatsu, Shiga, Japan). The V4 region of bacterial 16S rRNA gene was amplified with the 515F (5′-GTGYCAGCMGCCGCGGTAA-3′) and 806R (5′-GGACTACNVGGGTWTCTAAT-3′) primer set[83]. The PCR mixture (20 μL) contained 1× Ex Taq buffer, 0.2 mM dNTP mixture, 0.05 U Ex Taq HS (Takara Bio, Kusatsu, Shiga, Japan), 0.5 μM forward and reverse primers, 1 μM chloroplast and mitochondria peptide–nucleic acid clumps (to minimize the amplification of chloroplast and mitochondrial 16S rRNA genes from host plants[84]), and 1 μL of the template. PCR was performed as follows: 45 s at 95°C, 28 cycles of 15 s at 95°C, 10 s at 78°C, 30 s at 50°C, 30 s at 72°C, and 5 min at

bioRxiv preprint doi: https://doi.org/10.1101/2025.05.04.652152; this version posted May 6, 2025. The copyright holder for this preprint (which was not certified by peer review) is the author/funder, who has granted bioRxiv a license to display the preprint in perpetuity. It is made available under a CC-BY 4.0 International license.

72°C. The ITS2 region of fungal DNA was amplified with the fITS9 (5′-GAACACAGCGAAATGTGA-3′) and ITS4ngsUni (5′-CCTSCSCTTANTDATATGC-3′) primer set[85,86]. The PCR mixture was as described above except that peptide–nucleic acid clumps were omitted. PCR was performed as above except that the cycles at 78°C were omitted. The second PCR was then performed to add adapter sequences to amplicons. The PCR mixture (20 µL) contained 1× Ex Taq buffer, 0.2 mM dNTP Mixture, 0.05 U Ex Taq HS, 0.5 µM forward and reverse adapters, and 14 µL amplicons from the first PCR. PCR was performed as follows: 45 s at 95°C, 8 cycles of 15 s at 95°C, 30 s at 50°C, 30 s at 72°C, and 5 min at 72°C. Amplicons were purified using NucleoMag NGS Clean-up and Size Select magnetic beads (Macherey-Nagel, Dueren, Germany) following the manufacturer's protocol. DNA concentration of each sample was measured using Qubit dsDNA Quantification Assay Kits (Thermo Fisher Scientific, Waltham, MA, USA), and an approximately equimolar pool of amplicons was constructed. This pool was commercially sequenced using the Illumina MiSeq platform with the MiSeq Reagent Kit v3 for 2 × 300 bp paired-end reads in a single run (Macrogen, Tokyo, Japan).

Amplicon sequence processing, ASV classification, and taxonomic assignment

Amplicon sequencing yielded 15,561,772 total raw reads. Sequencing data were analyzed in QIIME 2 v2023.9[87]. Primer sequences of the V4 regions of the 16S rRNA gene and ITS2 region were removed from the 5′ ends of both forward and reverse reads, resulting in a total of 8,467,176 bacterial and 6,799,366 fungal trimmed reads. Quality filtering, chimera

bioRxiv preprint doi: https://doi.org/10.1101/2025.05.04.652152; this version posted May 6, 2025. The copyright holder for this preprint (which was not certified by peer review) is the author/funder, who has granted bioRxiv a license to display the preprint in perpetuity. It is made available under a CC-BY 4.0 International license.

361 removal, and inference of ASVs were performed using the DADA2 pipeline[88]. Bacterial
362 ASVs were inferred from paired-end sequences and fungal ASVs were inferred from single-
363 end sequences, yielding 7,073,527 bacterial and 6,252,014 fungal denoised reads. Taxonomy
364 was assigned to each bacterial ASV using a naïve Bayes classifier[89,90] based on the SILVA
365 database[91]. The ASVs assigned to chloroplasts or mitochondria and ASVs for which no taxa
366 were assigned at the kingdom level were excluded. Taxonomy was assigned to each fungal
367 ASV using BLAST+[92] based on the UNITE database[93]. The ASVs assigned to taxa other than
368 fungi at the kingdom level and ASVs that were not assigned to any taxa at the kingdom level
369 were excluded. A total of 3,465,682 filtered bacterial reads (32,090 ± 13,829 reads per
370 sample, mean ± SD) and 5,547,104 filtered fungal reads (51,362 ± 12946 reads per sample,
371 mean ± SD) were used in subsequent analyses.
372
373 **Collection of terpenes emitted by Japanese cedar**
374 We collected BVOCs emitted by cedar trees grown in the common garden at Kawatabi Field
375 Center in June 2023; the trees originated from three populations: Ajigasawa (n = 9), Azouji
376 (n = 10), and Yakushima (n = 6). The dynamic branch enclosure system[94] was used for
377 BVOC collection according to Hiura et al.[50], except that ambient air was used as the purge
378 gas instead of compressed air from gas cylinders. Briefly, intact branches were enclosed in a
379 Teflon bag with a purge air inlet that supplied ambient air, from which volatile organic
380 compounds and ozone had been removed by charcoal filters. Two air samples (2 L each) per
381 enclosure were collected simultaneously in adsorbent tubes: one for MT measurements and

bioRxiv preprint doi: https://doi.org/10.1101/2025.05.04.652152; this version posted May 6, 2025. The copyright holder for this preprint (which was not certified by peer review) is the author/funder, who has granted bioRxiv a license to display the preprint in perpetuity. It is made available under a CC-BY 4.0 International license.

382 the other one for SQTs and DTs. We followed Hiura et al.[50] for the analysis of the collected
383 terpenes. Briefly, MT samples were analyzed using a custom-built thermal desorption unit
384 coupled to a gas chromatograph (GC) equipped with a mass selective detector (MSD) and a
385 flame ionization detector (FID) (Agilent 6890/5973, Agilent, Santa Clara, US). SQT and DT
386 samples were analyzed using a GC/MSD (Agilent 6890/5973, Agilent, Santa Clara, US)
387 following solvent extraction and concentration.

388 To standardize emission rates, we applied the G93 model[95] and converted the measured
389 emission rates to basal emission rates, which were defined as the emission rates at a standard
390 leaf temperature of 30 °C, using the values of the constant β for models of the rates of terpene
391 emission by *C. japonica* reported previously[48,96]. For statistical analysis, the basal emission
392 rates were log-transformed after adding 0.01 (<1/100th of the lowest measured basal
393 emission rate) to avoid zero or negative values. Data of emitted terpenes are shown in
394 Supplementary Table S3.
395

396 **Acquisition and analysis of climatic data at the original locations of the wild Japanese**
397 **cedar populations**

398 The following climate data at the original locations of the wild populations of *C. japonica* for
399 1981–2010 were obtained from the CHELSA database[59–62]: annual mean temperature (bio1),
400 standard deviation of the monthly mean temperatures (bio4), annual precipitation (bio12),
401 coefficient of variation of the monthly precipitation estimates (bio15), mean monthly near-
402 surface relative humidity (hurs_mean), mean monthly potential evaporation

bioRxiv preprint doi: https://doi.org/10.1101/2025.05.04.652152; this version posted May 6, 2025. The copyright holder for this preprint (which was not certified by peer review) is the author/funder, who has granted bioRxiv a license to display the preprint in perpetuity. It is made available under a CC-BY 4.0 International license.

(pet_penman_mean), monthly mean temperatures (tas01–12), and monthly precipitation (pr01–12). The sum of the monthly precipitation for the months with mean temperatures below 0 °C was calculated for each location and used as an index of snowfall (snow). This index and the six average climatic variables other than the monthly means were summarized into PCs by PCA using the prcomp function in R v4.3.3[97].

Statistical analysis

Data analysis and visualization were performed using the tidyverse[98], phyloseq[99], vegan[100], MASS[101], and ggplot2[102] packages in R v4.3.3[97]. Using the vegan[100] package, the ASV table was rarefied to the minimum reads per sample to ensure equal sequencing depth (bacteria: 9,099 reads, fungi: 17,427 reads). The ASV richness of bacteria and fungi was calculated using the specnumber function in the vegan[100] package. Bray–Curtis dissimilarities among the microbial communities were calculated to measure their beta diversity using the vegan[100] package. Nonmetric multidimensional scaling (NMDS) based on Bray–Curtis dissimilarities was performed to visualize beta diversity. A permutational multivariate analysis of variance (PERMANOVA) with the Bray–Curtis dissimilarities as the response variable was performed to test for differences in microbial community composition among common gardens and populations, which were included together with their interactions as explanatory variables in the test. PERMANOVA was also performed using the climatic PC1 and PC2 at the origin sites of host individuals as explanatory variables instead of their populations to test for correlation between microbial community composition and climate at the origin sites of host

bioRxiv preprint doi: https://doi.org/10.1101/2025.05.04.652152; this version posted May 6, 2025. The copyright holder for this preprint (which was not certified by peer review) is the author/funder, who has granted bioRxiv a license to display the preprint in perpetuity. It is made available under a CC-BY 4.0 International license.

424 individuals. The list of fungal pathogens of Japanese cedar throughout Japan was obtained
425 from Kobayashi[63]. Fungal ASVs of the same genus as pathogens in the list were selected as
426 putative pathogenic fungi. To explore the drivers of the total relative abundances of the
427 putative pathogenic fungi, a negative binomial generalized linear model was fitted with the
428 aggregated abundances of these fungi after rarefaction as the response variable using the
429 glm.nb function with a log link function in the MASS[101] package. The climatic PC1 and PC2
430 at the origin sites of host individuals and common garden locations were included in the
431 model as explanatory variables. The significance of the explanatory variables was tested by
432 the Wald test.

433 To analyze the terpene emission profiles of Japanese cedar, we performed PCA of the
434 basal emission rates of terpenes after log transformation using the prcomp function. To
435 investigate the relationship between the terpene emission profile and the local climate at the
436 origin sites of the cedar trees, we fitted linear regression models with the terpene PCs as the
437 response variable. Simple linear regression models were fitted with either the terpene PC1 or
438 PC2 as the response variable and either the climatic PC1 or PC2 at the origin as the
439 explanatory variable, resulting in four models. The significance of the explanatory variables
440 in each model was tested by Student's *t*-test.

441 The following procedure was used to analyze the relationship between the basal terpene
442 emission rate and phyllosphere microbial community composition. First, to avoid a large
443 distortion of the entire NMDS plot due to the microbial community outliers, we detected

bioRxiv preprint doi: https://doi.org/10.1101/2025.05.04.652152; this version posted May 6, 2025. The copyright holder for this preprint (which was not certified by peer review) is the author/funder, who has granted bioRxiv a license to display the preprint in perpetuity. It is made available under a CC-BY 4.0 International license.

444 them using CLOUD analysis[103], a non-parametric test that is based on a distance matrix
445 between microbial communities and detects microbial samples whose mean distance to
446 neighbors is significantly different from those of other samples. Outliers in the bacterial and
447 fungal communities were detected using the mean Bray–Curtis dissimilarity to five
448 neighbors. The only detected outlier (the fungal community of one tree from the Azouji
449 population) was excluded from the subsequent analysis. Next, NMDS based on the Bray–
450 Curtis dissimilarities was performed only for those individuals from which emitted terpenes
451 were collected. Correlation was then tested between the NMDS coordinates constructed from
452 the phyllosphere microbial community compositions and the basal emission rates of terpenes
453 by vector fitting in the vegan package[100]. The basal emission rate of each terpene, their total
454 sum, or the sum for each category (i.e., MT or SQT) was used for the vector fitting after log
455 transformation. The sum for DT was not used for the analysis since only one tree emitted it.
456 Correlation was also tested between the abundances of bacterial phyla or fungal classes and
457 the NMDS coordinates constructed from the community compositions by vector fitting.
458
459 **Data availability**
460 The datasets generated and analysed during the current study are available in the DDBJ
461 Sequence Read Archive under the accession number PRJDB20421. All R scripts used for the
462 data analysis are available on GitHub (https://github.com/Satoyoshi-
463 ISHIZAKI/CedarPhyllosphere_SciRepo.git).

bioRxiv preprint doi: https://doi.org/10.1101/2025.05.04.652152; this version posted May 6, 2025. The copyright holder for this preprint (which was not certified by peer review) is the author/funder, who has granted bioRxiv a license to display the preprint in perpetuity. It is made available under a CC-BY 4.0 International license.

464

465 **References**

466 1. Vorholt, J. A. Microbial life in the phyllosphere. *Nat. Rev. Microbiol.* **10**, 828–840
467 (2012).

468 2. Mansfield, J. *et al.* Top 10 plant pathogenic bacteria in molecular plant pathology. *Mol.*
469 *Plant Pathol.* **13**, 614–629 (2012).

470 3. Humphrey, P. T., Nguyen, T. T., Villalobos, M. M. & Whiteman, N. K. Diversity and
471 abundance of phyllosphere bacteria are linked to insect herbivory. *Mol. Ecol.* **23**, 1497–
472 1515 (2014).

473 4. Innerebner, G., Knief, C. & Vorholt, J. A. Protection of *Arabidopsis thaliana* against
474 leaf-pathogenic *Pseudomonas syringae* by *Sphingomonas* strains in a controlled model
475 system. *Appl. Environ. Microbiol.* **77**, 3202–3210 (2011).

476 5. Ritpitakphong, U. *et al.* The microbiome of the leaf surface of *Arabidopsis* protects
477 against a fungal pathogen. *New Phytol.* **210**, 1033–1043 (2016).

478 6. De Zélicourt, A. *et al.* Ethylene induced plant stress tolerance by *Enterobacter* sp. SA187
479 is mediated by 2-keto-4-methylthiobutyric acid production. *PLOS Genet.* **14**, e1007273
480 (2018).

481 7. Nakano, M., Omae, N. & Tsuda, K. Inter-organismal phytohormone networks in plant-
482 microbe interactions. *Curr. Opin. Plant Biol.* **68**, 102258 (2022).

bioRxiv preprint doi: https://doi.org/10.1101/2025.05.04.652152; this version posted May 6, 2025. The copyright holder for this preprint (which was not certified by peer review) is the author/funder, who has granted bioRxiv a license to display the preprint in perpetuity. It is made available under a CC-BY 4.0 International license.

8. Pang, Z. *et al.* Linking plant secondary metabolites and plant microbiomes: a review. *Front. Plant Sci.* **12**, 621276 (2021).

9. Wang, Y., Pruitt, R. N., Nürnberger, T. & Wang, Y. Evasion of plant immunity by microbial pathogens. *Nat. Rev. Microbiol.* **20**, 449–464 (2022).

10. Hammerbacher, A., Coutinho, T. A. & Gershenzon, J. Roles of plant volatiles in defence against microbial pathogens and microbial exploitation of volatiles. *Plant Cell Environ.* **42**, 2827–2843 (2019).

11. Rico, L., Ogaya, R., Terradas, J. & Peñuelas, J. Community structures of N_2 -fixing bacteria associated with the phyllosphere of a H olm oak forest and their response to drought. *Plant Biol.* **16**, 586–593 (2014).

12. Moreira, J. C. F. *et al.* Asymbiotic nitrogen fixation in the phyllosphere of the Amazon forest: changing nitrogen cycle paradigms. *Sci. Total Environ.* **773**, 145066 (2021).

13. Abanda-Nkpwatt, D., Musch, M., Tschiersch, J., Boettner, M. & Schwab, W. Molecular interaction between *Methylobacterium extorquens* and seedlings: growth promotion, methanol consumption, and localization of the methanol emission site. *J. Exp. Bot.* **57**, 4025–4032 (2006).

14. Crombie, A. T. *et al.* Poplar phyllosphere harbors disparate isoprene-degrading bacteria. *Proc. Natl. Acad. Sci.* **115**, 13081–13086 (2018).

bioRxiv preprint doi: https://doi.org/10.1101/2025.05.04.652152; this version posted May 6, 2025. The copyright holder for this preprint (which was not certified by peer review) is the author/funder, who has granted bioRxiv a license to display the preprint in perpetuity. It is made available under a CC-BY 4.0 International license.

15. Laforest-Lapointe, I., Paquette, A., Messier, C. & Kembel, S. W. Leaf bacterial diversity mediates plant diversity and ecosystem function relationships. *Nature* **546**, 145–147 (2017).

16. Sohrabi, R., Paasch, B. C., Liber, J. A. & He, S. Y. Phyllosphere microbiome. *Annu. Rev. Plant Biol.* **74**, 539–568 (2023).

17. Eberl, F., Hammerbacher, A., Gershenzon, J. & Unsicker, S. B. Leaf rust infection reduces herbivore-induced volatile emission in black poplar and attracts a generalist herbivore. *New Phytol.* **220**, 760–772 (2018).

18. Schafer, H., Myronova, N. & Boden, R. Microbial degradation of dimethylsulphide and related C1-sulphur compounds: organisms and pathways controlling fluxes of sulphur in the biosphere. *J. Exp. Bot.* **61**, 315–334 (2010).

19. Bringel, F. & Couée, I. Pivotal roles of phyllosphere microorganisms at the interface between plant functioning and atmospheric trace gas dynamics. *Front. Microbiol.* **06**, (2015).

20. Chen, T. *et al.* A plant genetic network for preventing dysbiosis in the phyllosphere. *Nature* **580**, 653–657 (2020).

21. Laforest-Lapointe, I., Messier, C. & Kembel, S. W. Host species identity, site and time drive temperate tree phyllosphere bacterial community structure. *Microbiome* **4**, 27 (2016).

bioRxiv preprint doi: https://doi.org/10.1101/2025.05.04.652152; this version posted May 6, 2025. The copyright holder for this preprint (which was not certified by peer review) is the author/funder, who has granted bioRxiv a license to display the preprint in perpetuity. It is made available under a CC-BY 4.0 International license.

520 22. Aydogan, E. L., Moser, G., Müller, C., Kämpfer, P. & Glaeser, S. P. Long-term warming
521 shifts the composition of bacterial communities in the phyllosphere of *Galium album* in
522 a permanent grassland field-experiment. *Front. Microbiol.* **9**, 144 (2018).

523 23. Almario, J. *et al.* The leaf microbiome of *Arabidopsis* displays reproducible dynamics
524 and patterns throughout the growing season. *mBio* **13**, e02825-21 (2022).

525 24. Gaube, P., Junker, R. R. & Keller, A. Changes amid constancy: flower and leaf
526 microbiomes along land use gradients and between bioregions. *Basic Appl. Ecol.* **50**, 1–
527 15 (2021).

528 25. Laforest-Lapointe, I., Messier, C. & Kembel, S. W. Tree leaf bacterial community
529 structure and diversity differ along a gradient of urban intensity. *mSystems* **2**, e00087-17
530 (2017).

531 26. Wagner, M. R. *et al.* Host genotype and age shape the leaf and root microbiomes of a
532 wild perennial plant. *Nat. Commun.* **7**, 12151 (2016).

533 27. Knief, C., Ramette, A., Frances, L., Alonso-Blanco, C. & Vorholt, J. A. Site and plant
534 species are important determinants of the *Methylobacterium* community composition in
535 the plant phyllosphere. *ISME J.* **4**, 719–728 (2010).

536 28. Xiong, C. *et al.* Host selection shapes crop microbiome assembly and network
537 complexity. *New Phytol.* **229**, 1091–1104 (2021).

bioRxiv preprint doi: https://doi.org/10.1101/2025.05.04.652152; this version posted May 6, 2025. The copyright holder for this preprint (which was not certified by peer review) is the author/funder, who has granted bioRxiv a license to display the preprint in perpetuity. It is made available under a CC-BY 4.0 International license.

538 29. Kembel, S. W. *et al.* Relationships between phyllosphere bacterial communities and plant
539 functional traits in a neotropical forest. *Proc. Natl. Acad. Sci.* **111**, 13715–13720 (2014).

540 30. Bodenhausen, N., Bortfeld-Miller, M., Ackermann, M. & Vorholt, J. A. A synthetic
541 community approach reveals plant genotypes affecting the phyllosphere microbiota.
542 *PLoS Genet.* **10**, e1004283 (2014).

543 31. Junker, R. R. & Tholl, D. Volatile organic compound mediated interactions at the plant-
544 microbe interface. *J. Chem. Ecol.* **39**, 810–825 (2013).

545 32. Lee, G. W., Chung, M.-S., Kang, M., Chung, B. Y. & Lee, S. Direct suppression of a rice
546 bacterial blight (*Xanthomonas oryzae* pv. *oryzae*) by monoterpene (*S*)-limonene.
547 *Protoplasma* **253**, 683–690 (2016).

548 33. Burdon, R. C. F., Junker, R. R., Scofield, D. G. & Parachnowitsch, A. L. Bacteria
549 colonising *Penstemon digitalis* show volatile and tissue-specific responses to a natural
550 concentration range of the floral volatile linalool. *Chemoecology* **28**, 11–19 (2018).

551 34. Riedlmeier, M. *et al.* Monoterpenes support systemic acquired resistance within and
552 between plants. *Plant Cell* **29**, 1440–1459 (2017).

553 35. Kleinheinz, G. T., Bagley, S. T., John, W. P. St., Rughani, J. R. & McGinnis, G. D.
554 Characterization of alpha-pinene-degrading microorganisms and application to a bench-
555 scale biofiltration system for VOC degradation. *Arch. Environ. Contam. Toxicol.* **37**,
556 151–157 (1999).

bioRxiv preprint doi: https://doi.org/10.1101/2025.05.04.652152; this version posted May 6, 2025. The copyright holder for this preprint (which was not certified by peer review) is the author/funder, who has granted bioRxiv a license to display the preprint in perpetuity. It is made available under a CC-BY 4.0 International license.

557 36. DiGuistini, S. *et al.* Genome and transcriptome analyses of the mountain pine beetle-
558 fungal symbiont *Grosmannia clavigera*, a lodgepole pine pathogen. *Proc. Natl. Acad.*
559 *Sci.* **108**, 2504–2509 (2011).

560 37. Scala, A. *et al. E*-2-hexenal promotes susceptibility to *Pseudomonas syringae* by
561 activating jasmonic acid pathways in *Arabidopsis*. *Front. Plant Sci.* **4**, (2013).

562 38. Shen, Q., Liu, L., Wang, L. & Wang, Q. Indole primes plant defense against necrotrophic
563 fungal pathogen infection. *PLOS ONE* **13**, e0207607 (2018).

564 39. Gaube, P. *et al.* Inter- and intraspecific phytochemical variation correlate with epiphytic
565 flower and leaf bacterial communities. *Environ. Microbiol.* **25**, 1624–1643 (2023).

566 40. Junker, R. R. *et al.* Composition of epiphytic bacterial communities differs on petals and
567 leaves. *Plant Biol.* **13**, 918–924 (2011).

568 41. Junker, R. R. *et al.* Covariation and phenotypic integration in chemical communication
569 displays: biosynthetic constraints and eco-evolutionary implications. *New Phytol.* **220**,
570 739–749 (2018).

571 42. Fitzky, A. C. *et al.* Diversity and interrelations among the constitutive VOC emission
572 blends of four broad-leaved tree species at seedling stage. *Front. Plant Sci.* **12**, 708711
573 (2021).

574 43. Laothawornkitkul, J., Taylor, J. E., Paul, N. D. & Hewitt, C. N. Biogenic volatile organic
575 compounds in the Earth system. *New Phytol.* **183**, 27–51 (2009).

bioRxiv preprint doi: https://doi.org/10.1101/2025.05.04.652152; this version posted May 6, 2025. The copyright holder for this preprint (which was not certified by peer review) is the author/funder, who has granted bioRxiv a license to display the preprint in perpetuity. It is made available under a CC-BY 4.0 International license.

576 44. Carslaw, K. S. *et al.* A review of natural aerosol interactions and feedbacks within the
577 Earth system. *Atmospheric Chem. Phys.* **10**, 1701–1737 (2010).

578 45. Guenther, A. B. *et al.* The model of emissions of gases and aerosols from nature version
579 2.1 (MEGAN2.1): an extended and updated framework for modeling biogenic
580 emissions. *Geosci. Model Dev.* **5**, 1471–1492 (2012).

581 46. Tsumura, Y. Review: Genetic structure and local adaptation in natural forests of
582 *Cryptomeria japonica*. *Ecol. Res.* **38**, 64–73 (2023).

583 47. Forestry Agency of Japan. *2011 forestry census*. (Forestry Agency, 2011).

584 48. Matsunaga, S. N. *et al.* Determination and potential importance of diterpene (kaur-16-
585 ene) emitted from dominant coniferous trees in Japan. *Chemosphere* **87**, 886–893
586 (2012).

587 49. Miyama, T. *et al.* Seasonal changes in interclone variation following ozone exposure on
588 three major gene pools: an analysis of *Cryptomeria japonica* clones. *Atmosphere* **10**,
589 643 (2019).

590 50. Hiura, T. *et al.* Diversification of terpenoid emissions proposes a geographic structure
591 based on climate and pathogen composition in Japanese cedar. *Sci. Rep.* **11**, 8307
592 (2021).

593 51. Dada, L. *et al.* Role of sesquiterpenes in biogenic new particle formation. *Sci. Adv.* **9**,
594 eadi5297 (2023).

bioRxiv preprint doi: https://doi.org/10.1101/2025.05.04.652152; this version posted May 6, 2025. The copyright holder for this preprint (which was not certified by peer review) is the author/funder, who has granted bioRxiv a license to display the preprint in perpetuity. It is made available under a CC-BY 4.0 International license.

595 52. Luo, Y. *et al.* Oxidation product characterization from ozonolysis of the diterpene *ent*-
596 kaurene. *Atmospheric Chem. Phys.* **22**, 5619–5637 (2022).

597 53. Tsumura, Y. *et al.* Genetic differentiation and evolutionary adaptation in *Cryptomeria*
598 *japonica*. *G3* **4**, 2389–2402 (2014).

599 54. Moriguchi, N. *et al.* Inferring the demographic history of Japanese cedar, *Cryptomeria*
600 *japonica*, using amplicon sequencing. *Heredity* **123**, 371–383 (2019).

601 55. Tsumura, Y. *et al.* Effects of the last glacial period on genetic diversity and genetic
602 differentiation in *Cryptomeria japonica* in East Asia. *Tree Genet. Genomes* **16**, 19
603 (2020).

604 56. Ohta, T., Niwa, S. & Hiura, T. Geographical variation in Japanese cedar shapes soil
605 nutrient dynamics and invertebrate community. *Plant Soil* **437**, 355–373 (2019).

606 57. Azuma, W. A., Kawai, K., Tanabe, T., Nakahata, R. & Hiura, T. Intraspecific variation in
607 growth-related traits—from leaf to whole-tree—in three provenances of *Cryptomeria*
608 *japonica* canopy trees grown in a common garden. *Ecol. Res.* **38**, 83–97 (2023).

609 58. Nakahata, R., Azuma, W. A., Tanabe, T., Kawai, K. & Hiura, T. Genotypic variations
610 appear in fine root morphological traits of *Cryptomeria japonica* trees grown in a
611 common garden. *Ecol. Res.* **39**, 717–729 (2024).

612 59. Karger, D. N. *et al.* Climatologies at high resolution for the earth's land surface areas.
613 *Sci. Data* **4**, 170122 (2017).

bioRxiv preprint doi: https://doi.org/10.1101/2025.05.04.652152; this version posted May 6, 2025. The copyright holder for this preprint (which was not certified by peer review) is the author/funder, who has granted bioRxiv a license to display the preprint in perpetuity. It is made available under a CC-BY 4.0 International license.

614 60. Karger, D. N. *et al.* Climatologies at high resolution for the earth's land surface areas.
615 *EnviDat* https://doi.org/10.16904/envidat.228 (2021).

616 61. Brun, P., Zimmermann, N. E., Hari, C., Pellissier, L. & Karger, D. N. Global climate-
617 related predictors at kilometer resolution for the past and future. *Earth Syst. Sci. Data*
618 **14**, 5573–5603 (2022).

619 62. Brun, P., Zimmermann, N. E., Hari, C., Pellissier, L. & Karger, D. N. CHELSA-
620 BIOCLIM+ A novel set of global climate-related predictors at kilometre-resolution.
621 *EnviDat* https://doi.org/10.16904/envidat.332 (2022).

622 63. Kobayashi, T. *Index of fungi inhabiting woody plants in Japan −Host, Distribution and*
623 *Literature*. (Zenkoku-Noson-Kyoiku Kyokai, 2007).

624 64. Bálint, M. *et al.* Host genotype shapes the foliar fungal microbiome of balsam poplar
625 (*Populus balsamifera*). *PLoS ONE* **8**, e53987 (2013).

626 65. Coince, A. *et al.* Leaf and root-associated fungal assemblages do not follow similar
627 elevational diversity patterns. *PLoS ONE* **9**, e100668 (2014).

628 66. Fukasawa, Y. & Matsuoka, S. Communities of wood-inhabiting fungi in dead pine logs
629 along a geographical gradient in Japan. *Fungal Ecol.* **18**, 75–82 (2015).

630 67. Tedersoo, L. *et al.* Global diversity and geography of soil fungi. *Science* **346**, 1256688
631 (2014).

bioRxiv preprint doi: https://doi.org/10.1101/2025.05.04.652152; this version posted May 6, 2025. The copyright holder for this preprint (which was not certified by peer review) is the author/funder, who has granted bioRxiv a license to display the preprint in perpetuity. It is made available under a CC-BY 4.0 International license.

632 68. Junker, R. R., He, X., Otto, J.-C., Ruiz-Hernández, V. & Hanusch, M. Divergent
633 assembly processes? A comparison of the plant and soil microbiome with plant
634 communities in a glacier forefield. *FEMS Microbiol. Ecol.* **97**, fiab135 (2021).

635 69. Labouyrie, M. *et al.* Patterns in soil microbial diversity across Europe. *Nat. Commun.* **14**,
636 3311 (2023).

637 70. Martin, D. M., Gershenzon, J. & Bohlmann, J. Induction of volatile terpene biosynthesis
638 and diurnal emission by methyl jasmonate in foliage of Norway spruce. *Plant Physiol.*
639 **132**, 1586–1599 (2003).

640 71. Schnee, C., Gershenzon, J. & Degenhardt, J. The maize gene *terpene synthase 1* encodes
641 a sesquiterpene synthase catalyzing the formation of (*E*)-*β*-farnesene, (*E*)-nerolidol, and
642 (*E*, *E*)-farnesol after herbivore damage. *Plant Physiol.* **130**, 2049–2060 (2002).

643 72. Piesik, D., Wenda-Piesik, A., Weaver, D. K. & Morrill, W. L. Influence of *Fusarium*
644 crown rot disease on semiochemical production by wheat plants. *J. Phytopathol.* **155**,
645 488–496 (2007).

646 73. Pieterse, C. M. J., Poelman, E. H., Van Wees, S. C. M. & Dicke, M. Induced plant
647 responses to microbes and insects. *Front. Plant Sci.* **4**, (2013).

648 74. Gupta, R. *et al.* Cytokinin drives assembly of the phyllosphere microbiome and promotes
649 disease resistance through structural and chemical cues. *ISME J.* **16**, 122–137 (2022).

bioRxiv preprint doi: https://doi.org/10.1101/2025.05.04.652152; this version posted May 6, 2025. The copyright holder for this preprint (which was not certified by peer review) is the author/funder, who has granted bioRxiv a license to display the preprint in perpetuity. It is made available under a CC-BY 4.0 International license.

650 75. Saito, T., Kusumoto, N. & Hiura, T. Relation of leaf terpene contents to terpene emission
651 profiles in Japanese cedar (*Cryptomeria japonica*). *Ecol. Res.* **38**, 74–82 (2023).

652 76. Rodrigues, M. G. & Fonseca, Á. Molecular systematics of the dimorphic ascomycete
653 genus *Taphrina*. *Int. J. Syst. Evol. Microbiol.* **53**, 607–616 (2003).

654 77. Tsai, I. J. *et al.* Comparative genomics of *Taphrina* fungi causing varying degrees of
655 tumorous deformity in plants. *Genome Biol. Evol.* **6**, 861–872 (2014).

656 78. Vacher, C. *et al.* The phyllosphere: microbial jungle at the plant–climate interface. *Annu.*
657 *Rev. Ecol. Evol. Syst.* **47**, 1–24 (2016).

658 79. Peay, K. G., Bruns, T. D., Kennedy, P. G., Bergemann, S. E. & Garbelotto, M. A strong
659 species–area relationship for eukaryotic soil microbes: island size matters for
660 ectomycorrhizal fungi. *Ecol. Lett.* **10**, 470–480 (2007).

661 80. Van Der Gucht, K. *et al.* The power of species sorting: local factors drive bacterial
662 community composition over a wide range of spatial scales. *Proc. Natl. Acad. Sci.* **104**,
663 20404–20409 (2007).

664 81. Jumpponen, A. & Jones, K. L. Seasonally dynamic fungal communities in the *Quercus*
665 *macrocarpa* phyllosphere differ between urban and nonurban environments. *New*
666 *Phytol.* **186**, 496–513 (2010).

667 82. Tian, X. *et al.* Template preparation affects 16S rRNA high-throughput sequencing
668 analysis of phyllosphere microbial communities. *Front. Plant Sci.* **8**, 1623 (2017).

bioRxiv preprint doi: https://doi.org/10.1101/2025.05.04.652152; this version posted May 6, 2025. The copyright holder for this preprint (which was not certified by peer review) is the author/funder, who has granted bioRxiv a license to display the preprint in perpetuity. It is made available under a CC-BY 4.0 International license.

669 83. Caporaso, J. G. *et al.* Global patterns of 16S rRNA diversity at a depth of millions of
670 sequences per sample. *Proc. Natl. Acad. Sci.* **108**, 4516–4522 (2011).

671 84. Lundberg, D. S., Yourstone, S., Mieczkowski, P., Jones, C. D. & Dangl, J. L. Practical
672 innovations for high-throughput amplicon sequencing. *Nat. Methods* **10**, 999–1002
673 (2013).

674 85. Ihrmark, K. *et al.* New primers to amplify the fungal ITS2 region − evaluation by 454-
675 sequencing of artificial and natural communities. *FEMS Microbiol. Ecol.* **82**, 666–677
676 (2012).

677 86. Tedersoo, L. & Lindahl, B. Fungal identification biases in microbiome projects. *Environ.*
678 *Microbiol. Rep.* **8**, 774–779 (2016).

679 87. Bolyen, E. *et al.* Reproducible, interactive, scalable and extensible microbiome data
680 science using QIIME 2. *Nat. Biotechnol.* **37**, 852–857 (2019).

681 88. Callahan, B. J. *et al.* DADA2: high-resolution sample inference from Illumina amplicon
682 data. *Nat. Methods* **13**, 581–583 (2016).

683 89. Bokulich, N. A. *et al.* Optimizing taxonomic classification of marker-gene amplicon
684 sequences with QIIME 2's q2-feature-classifier plugin. *Microbiome* **6**, 90 (2018).

685 90. Robeson, M. S. *et al.* RESCRIPt: reproducible sequence taxonomy reference database
686 management. *PLOS Comput. Biol.* **17**, e1009581 (2021).

bioRxiv preprint doi: https://doi.org/10.1101/2025.05.04.652152; this version posted May 6, 2025. The copyright holder for this preprint (which was not certified by peer review) is the author/funder, who has granted bioRxiv a license to display the preprint in perpetuity. It is made available under a CC-BY 4.0 International license.

687 91. Quast, C. *et al.* The SILVA ribosomal RNA gene database project: improved data
688 processing and web-based tools. *Nucleic Acids Res.* **41**, D590–D596 (2012).

689 92. Camacho, C. *et al.* BLAST+: architecture and applications. *BMC Bioinformatics* **10**, 421
690 (2009).

691 93. Abarenkov, K. *et al.* The UNITE database for molecular identification and taxonomic
692 communication of fungi and other eukaryotes: sequences, taxa and classifications
693 reconsidered. *Nucleic Acids Res.* **52**, D791–D797 (2024).

694 94. Ortega, J. & Helmig, D. Approaches for quantifying reactive and low-volatility biogenic
695 organic compound emissions by vegetation enclosure techniques – Part A.
696 *Chemosphere* **72**, 343–364 (2008).

697 95. Guenther, A. B., Zimmerman, P. R., Harley, P. C., Monson, R. K. & Fall, R. Isoprene
698 and monoterpene emission rate variability: model evaluations and sensitivity analyses.
699 *J. Geophys. Res. Atmospheres* **98**, 12609–12617 (1993).

700 96. Matsunaga, S. N. *et al.* Monoterpene and sesquiterpene emissions from Sugi
701 (*Cryptomeria japonica*) based on a branch enclosure measurements. *Atmospheric*
702 *Pollut. Res.* **2**, 16–23 (2011).

703 97. R Core Team. R: a language and environment for statistical computing. https://www.R-
704 project.org/ (R Foundation for Statistical Computing, Vienna, Austria, 2024).

705 98. Wickham, H. *et al.* Welcome to the tidyverse. *J. Open Source Softw.* **4**, 1686 (2019).

bioRxiv preprint doi: https://doi.org/10.1101/2025.05.04.652152; this version posted May 6, 2025. The copyright holder for this preprint (which was not certified by peer review) is the author/funder, who has granted bioRxiv a license to display the preprint in perpetuity. It is made available under a CC-BY 4.0 International license.

706 99. McMurdie, P. J. & Holmes, S. phyloseq: an R package for reproducible interactive
707 analysis and graphics of microbiome census data. *PLoS ONE* **8**, e61217 (2013).

708 100. Oksanen, J. *et al.* vegan: Community Ecology Package, Version 2.6-8. https://cran.r-
709 project.org/package=vegan (2024).

710 101. Venables, W. N. & Ripley, B. D. *Modern applied statistics with S*. (Springer, 2002).

711 102. Wickham, H. *ggplot2: Elegant graphics for data analysis.* (Springer Verlag, New York,
712 2016).

713 103. Montassier, E. *et al.* CLOUD: a non-parametric detection test for microbiome outliers.
714 *Microbiome* **6**, 137 (2018).

715

716

bioRxiv preprint doi: https://doi.org/10.1101/2025.05.04.652152; this version posted May 6, 2025. The copyright holder for this preprint (which was not certified by peer review) is the author/funder, who has granted bioRxiv a license to display the preprint in perpetuity. It is made available under a CC-BY 4.0 International license.

Figure legends

Fig. 1. Compositions of the phyllosphere microbial communities of Japanese cedars planted in the common gardens. Each bar represents the phyllosphere microbial community of each individual at (**A, C**) Kawatabi and (**B, D**) Tsukuba. Bar arrangement is based on the value of the climatic PC1 (from high to low) at the origin site of each individual. (**A, B**) Relative abundances of eight most abundant bacterial phyla. (**C, D**) Relative abundances of eight most abundant fungal classes. The original population of each sample is indicated under the bar (see Supplementary Fig. S1 and Table S1 for the names and locations).

Fig. 2. Differences in the composition of the phyllosphere (**A**) bacterial and (**B**) fungal communities of Japanese cedar between the common gardens at Kawatabi (blue) and Tsukuba (orange). Differences were visualized using nonmetric multidimensional scaling (NMDS) based on Bray–Curtis dissimilarities. The density of color represents the climatic PC1 at the origin site of each tree. MDS1 indicates the first ordination axis generated by NMDS and MDS2 indicates the second.

Fig. 3. Relationship between the abundance of the putative pathogenic fungi after rarefaction and climatic PC1 at the origin sites of the host trees. The abundances of the fungi are displayed. They were aggregated on the basis of their putative functional groups (color of the points). The solid line represents fitted values from a negative binomial generalized linear

bioRxiv preprint doi: https://doi.org/10.1101/2025.05.04.652152; this version posted May 6, 2025. The copyright holder for this preprint (which was not certified by peer review) is the author/funder, who has granted bioRxiv a license to display the preprint in perpetuity. It is made available under a CC-BY 4.0 International license.

737 model, where the aggregated abundance of all guilds was modeled as a function of climatic
738 PC1. Shaded areas indicate the 95% confidence intervals of the model predictions.
739
740 **Fig. 4.** Terpene emission profiles of Japanese cedar in the common garden at Kawatabi. (**A**)
741 Basal emission rates of monoterpenes (green to yellow), a sesquiterpene (purple), and a
742 diterpene (blue) emitted from each cedar individual originating from three populations. (**B**)
743 Principal component analysis of log-transformed basal emission rates of terpenes.
744
745 **Fig. 5.** Vector fitting of log-transformed basal emission rates of terpenes onto NMDS
746 coordinates constructed from the compositions of the phyllosphere (**A**) bacterial and (**B**)
747 fungal communities of Japanese cedar from three populations (blue: Ajigasawa, grey: Azouji,
748 orange: Yakushima). (**A**) Bacterial phyla and (**B**) fungal classes whose relative abundances
749 were significantly correlated with the NMDS coordinates are also shown. Only loading
750 vectors of significantly correlated terpenes and microbial taxa are shown (solid: $p < 0.05$,
751 dashed: $p < 0.1$).
752
753 **Acknowledgements**
754 This research was partly supported by the Japan Society for the Promotion of Science to
755 T.I.K. (No. 22H05715), Y.S. (No. 23H04970), and T.H. (Nos. 21H02227, 21H05316,

bioRxiv preprint doi: https://doi.org/10.1101/2025.05.04.652152; this version posted May 6, 2025. The copyright holder for this preprint (which was not certified by peer review) is the author/funder, who has granted bioRxiv a license to display the preprint in perpetuity. It is made available under a CC-BY 4.0 International license.

24K01809). We thank the staff of Kawatabi Field Science Center, Tohoku University and Mountain Science Center, University of Tsukuba for supporting our fieldwork.

Author contributions

S.I. performed statistical analysis and wrote the first draft; T.I.K and T.H. generated hypotheses and designed research; S.I. and T.I.K. collected and performed experiments with microbial samples; Y.O. sampled terpenes emitted from the Japanese cedars; Y.O. and T.S. analyzed the collected terpenes; Y.S. and Y.T. designed and maintained the common gardens. All authors participated in manuscript preparation.

Competing interests

The authors declare no competing interests.